

## Electrooxidation of Methanol on Carbon Supported Pt-Ru Nanocatalysts Prepared by Ethanol Reduction Method

A. B. Kashyout<sup>1,\*</sup>, Abu Bakr A.A. Nassr<sup>1,2</sup>, Leonardo Giorgi<sup>2</sup>, T. Maiyalagan<sup>3</sup>,  
Bayummy A. B. Youssef<sup>4</sup>

<sup>1</sup> Electronic Materials Department, Advanced Technology and New Materials Research Institute, Mubarak City for Scientific Research and Technology Applications, 21934 New Borg El-Arab City, Alexandria, Egypt.

<sup>2</sup> ENEA, Casaccia Research Centre, Department of Physical Technologies and New Materials, Via Anguillarese 301, 00123 S. Maria di Galeria, Rome, Italy

<sup>3</sup> Department of Chemistry, VIT University, Vellore-632014, India

<sup>4</sup> Department of Computer Based Engineering Applications, Informatics Research Institute, Mubarak City for Scientific Research and Technologies Applications, 21934 New Borg El-Arab City, Alexandria, Egypt

\*E-mail: [akashyout@mucsat.sci.eg](mailto:akashyout@mucsat.sci.eg)

*Received:* 26 January 2010 / *Accepted:* 1 December 2010 / *Published:* 1 February 2011

---

Carbon Supported PtRu nanocatalysts have been prepared by simple impregnation reduction method in which Pt and Ru precursors are reduced by ethanol under reflux conditions for different reaction times. The prepared nanocatalysts were characterized by means of XRD, EDAX, ICP-AAS, FESEM and TEM. XRD analyses showed that all nanocatalysts exhibited f.c.c crystal structure, the structure characteristic for pure Pt, except for that reduced at prolonged reaction time of 4h which showed the presence of characteristic peak for Ru metal. The lattice constant calculations indicate that all catalysts are present in unalloyed phase and the average particle size as determined by TEM was in the range of 3.7 nm. The electrocatalytic activities and stability for the prepared nanocatalysts methanol electro-oxidation reaction (MOR) were studied by cyclic voltammetry. The catalysts prepared at 2h reduction time showed higher electrocatalytic activity in terms of mass specific activity and good stability over potential sweep for 100 cycles for methanol electro-oxidation. The results showed that the prepared nanocatalysts are considered as promising electrode catalyst (anode catalyst) for electro-oxidation of methanol in direct methanol fuel cells.

---

**Keywords:** PtRu nanocatalysts, methanol electro-oxidation, cyclic voltammetry, DMFCs

## 1. INTRODUCTION

The electro-oxidation of small organic molecules on Pt electrocatalysts based electrodes has received more attention in the last decades due their application for electrochemical energy conversion in direct liquid feed fuel cells [1-3]. Among these molecules; methanol is used as liquid fuel for direct methanol fuel cells (DMFCs). It has a higher electron density (six electron production during its electro-oxidation) and it has a good electrochemical activity due to the presence of electroactive hydroxyl group which can be attached or adsorbed to the electrode surface [4].

The electro-oxidation of methanol has been studied on many electrode fabricated from unsupported metals and metal supported onto different supporting materials. Pt catalysts are still the most active catalysts materials for electro-oxidation of methanol [3, 5-9]. The electro-oxidation of methanol on Pt electrode surface is combined with several steps of dehydrogenation to form CO which is oxidized into CO<sub>2</sub> [10, 11]. The poisoning of the electrode surface (anode) by CO molecules formed during the methanol oxidation is one of the obstacles in the development of DMFCs for commercial applications. The modification of Pt catalysts with other metals or metal oxides which have higher tendency to form surface oxygenated species at lower potential is considered as one of the best ways to solve this problem [12, 13]. In this regard, many efforts have been done by many groups to synthesis new catalysts systems for methanol oxidation based on bimetallic catalysts such as PtRu[14-17], PtSn[18,19], PtNi[20,21], PtMo[22,23], ternary alloy ; PtRuNi[24-26], PtRuMo[25,27,28], and PtMO<sub>x</sub> (where M is, Ti, V, Mn, W) [29-32].

Among all catalyst systems, PtRu catalysts prepared as nanoparticles have received more attention due to its high CO tolerance. The formation of surface oxygenated species on Ru takes place at a potential lower than that on Pt. So, the presence of Ru adjacent to Pt reduces the poisoning of Pt surface by CO [8,9]. In this catalyst system, Pt services as active sites for methanol adsorption and dehydrogenation while Ru serves as catalyst promoter on which CO is oxidized into CO<sub>2</sub>. This model mechanism is known as bifunctional mechanism. Other model is suggested based on electronic structure change upon addition of Ru. According to this model, the addition of Ru can change the electronic structure of catalyst surface which lead to decrease the bonding between the CO molecules and Pt catalyst surface [8, 9, 33].

Many research groups are working to explore preparation method for PtRu catalyst system [7]. The catalytic activity of the catalysts depends on their preparation methods. Also, the cost of catalysts preparation process should be taken into consideration for the application in fuel cells. Therefore; the searching for simple preparation methods with low cost and high catalytic activity will lead to the development of fuel cells industry.

Wet chemical method or some times called chemical impregnation method is considered as the most powerful method for preparation of catalysts nanoparticles specially; supported PtRu catalysts. The procedures for this method are easy and can be developed for large-scale production [7, 34]. In wet chemical method, the metal precursors are impregnated on the carbon support in aqueous or/and organic media followed by the reduction using reducing agent such as sodium borohydride, formic acid, hydrazine. Also, the organic alcohols (methanol, ethanol, isopropanol and ethylene glycol, glycerol and diethylene glycol) are known as good reducing agents for the preparation of PtRu and

other nanoparticles. Advantages of using alcohols as reducing agent are that there is no side reaction products can be obtained and the formation of relative pure nanoparticles are well synthesized [7,34,35].

The reduction process are carried out in presence of stabilizers such as PVA or other polymers or surfactant materials which serve as capping agent to prevent the particle agglomeration. In fact, these capping materials have adverse effect on the electrocatalytic activity, since these stabilizers are adsorbed on the surface of the nanoparticles catalysts and blocking the active sites available for the electrochemical reaction in addition to its lower electrical conductivity. Also, the removal of these protective agents by heat treatment may be has side-effect on the electrocatalytic activity due the change of crystal structure of the active phase in the catalysts or increase their particle size [36, 37].

Lee *et al.* prepared PtRu/C nanocataysts using ethanol reduction method and tested the prepared catalysts for methanol electrooxidation reaction [38]. The results showed that the preparation process has adverse effect on the electrocatalytic activity when carried out in alkaline media. Also, carbon supported Pt and PtAu catalysts as electrocatalysts for oxygen reduction reaction (ORR) have been prepared by ethanol reduction method in the presence of PVP as stabilizing and complexing agent. The reduction process were carried out in alkaline media. The removal of the stabilizing agent was carried out by heating the catalysts at high temperature in air followed by their reduction in flow of hydrogen at elevated temperature. The prepared electrocatalysts showed good electrocatalytic activity towards ORR [39].

In this work, we report a simple method for preparation of PtRu nanoparticles supported on carbon support (Vulcan XC-72R) by using ethanol as a reducing agent without using any stabilizers and no modification of the preparation media (pH) and without heat treatment. The prepared nanocatalysts are characterized by means of structural tools; XRD, FESEM and TEM and chemical analyses by EDAX and ICP-AAS. The electrocatalytic activity is tested for methanol electrooxidation by cyclic voltammetry technique. The effect of reduction time on the durability of the catalysts is also studied.

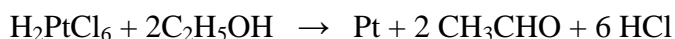
## 2. EXPERIMENTAL PART

### 2.1. Electrocatalyst Preparation

In this work, a carbon supported PtRu nanoparticles electrocatalyst with atomic ratio Pt:Ru (1:1) and 20% wt of metal loading (PtRu) on carbon was prepared according to the following procedures. 100 mg of carbon (Vulcan XC-72R) was dispersed in 20 ml ethanol in an ultrasonic bath for 15 min. To the above suspension; 34.6 mg of  $H_2PtCl_6$  dissolved in 5 ml water and 17.5 mg of  $RuCl_3$  dissolved in 5 ml of water were added and then 80 ml of ethanol was also added to the reaction mixture. The total mixture was kept under stirring for 1h followed by sonication in an ultrasonic bath for 30 min to insure the adsorption and dispersion of the metal precursors on the carbon support. The resulted mixture was heated under reflux at  $(80 \pm 2^\circ C)$  under stirring for different reaction times after which the reaction mixture was leaved to cool to room temperature and then centrifuged to separate the

catalysts powder. The catalysts were subjected to many cycles of washing with water and centrifuge until no  $\text{Cl}^-$  ions were detected (silver nitrite test) and then dried in vacuum oven at  $100^\circ\text{C}$  for 12h.

The reductive reactions can be represented by the following equations [38]:



The PtRu/C catalysts produced during this work are (PtRu/C1, PtRu/C2 and PtRu/C4). These labels are giving according to their reaction times of 1h, 2h and 4h; respectively.

## 2.2. Electrocatalyst Characterization

### 2.2.1. Physical and Chemical Characterization

The total metal loading was determined by ICP-AAS (Prodigy, high dispersion ICP, Leman). The measurement was carried out by collecting all the filtrates during the washing process and determining the concentration of Pt and Ru contents in the filtrate from which we can calculate the amount of metal loading on the carbon support. The chemical composition of the prepared catalysts was determined by the energy dispersive X-ray analysis (EDAX) combined with SEM (JEOL JSM 6360LA). X-ray diffraction study of the prepared nanocatalysts were carried out using (Schimadzu 7000) diffractometer, operating with Cu  $K\alpha$  radiation ( $\lambda=0.154060$  nm) generated at 30 kV and 30 mA with scanning rate of  $2^\circ \text{min}^{-1}$  for  $2\theta$  values between  $20$  and  $90^\circ$  degree. The nanocatalysts morphology and dispersion on the support and their particle size were investigated by FESEM (LEO 1530) and TEM (JEOL, 200CX). The samples were prepared by dispersion of the catalysts powder in ethanol and sonication, then the sample was deposited on a diamond polished graphite paper supported on aluminum sample holder for FESEM analysis and on carbon coated Cu grid for TEM analysis.

The average particle size and particle size distribution are acquired using FORTRAN code. The code has been made to apply the image processing rules on the TEM images of PtRu/C catalysts to determine exactly the average particle size and the particles size distribution from digital images.

The code design steps are removing the background (the carbon support), clustering the pixels which form each particle and finally computing the diameter of each particle [40]. Removing of background has been done using the threshold technique. For clustering of the pixels; the clustering based iterative method has been used. The method mainly depends on getting certain relation between each pixel and its neighbors. This relation is applied iteratively until the results of this relation have no variation with increasing the iteration:

1. Starting with two arrays (A, B) which have a number of elements. Each element is corresponding to each pixel of image.

2. Fill the arrays A and B with large number. This number must be greater than the expected particles number (LN)
3. Putting a variable N as counter for particle Number
4. Starting N=0
5. Calculating every array elements according the next relation:

$$B_{i,j} = \text{Min}(A_{i+1,j}, A_{i-1,j}, A_{i,j+1}, A_{i,j-1})$$

6. If  $A_{i,j}$  is equal to the larger number LN then  $N = N + 1$  and  $A_{i,j} = N$
7. If  $A_{i,j}$  is less than (LN),  $A_{i,j}$  remains unchanged
8. Getting  $r = |A - B|$
9. If r equal zero the solution is accomplished if not the program must execute steps 5,6,7,8,9 after putting  $A = B$

Finally, the array A contains the particle numbers corresponding to all pixels of the image. From the total number of pixel we calculated the area of each particle which subsequently used to calculate the particle size.

### 2.2.2. Electrochemical Measurements

The electrocatalytic activities of the prepared catalysts were evaluated towards methanol electrooxidation reaction (MOR) in a standard three electrodes electrochemical cell in which saturated calomel electrode (SCE) (0.241 vs. NHE) and high purity graphite electrode were used as reference electrode and counter electrode; respectively. The working electrode is glass carbon disc (GCD) electrode coated with the catalyst layer. The catalysts layer was prepared by mixing the catalyst powder with Nafion solution (10% Wt, DuPont), water and isopropanol and then sonicated in ultrasonic water bath for 15 min followed by magnetic stirring for 1h to form a catalyst ink which finally coated on GCD and dried for 20 min at 80 °C. The working electrode area was 0.79 cm<sup>2</sup> and the amount of catalysts loading (PtRu in mg/cm<sup>2</sup>) in the working electrode was controlled to be 0.2 mg/cm<sup>2</sup>. The measurements were carried out with EG&G 273A potentiostat/galvanostat from Princeton Applied Research (PAR) and controlled with Corware/Corview software (Scribner Associates). The electrode measurements were activated in 1M H<sub>2</sub>SO<sub>4</sub> by sweep the electrode between -0.28 – 1 V (SCE) with a scan rate of 100 mVs<sup>-1</sup> till the reproducible voltammogram was obtained (about 100 cycles). The electrocatalytic activity for methanol electro-oxidation was tested in 0.5 M CH<sub>3</sub>OH/1 M H<sub>2</sub>SO<sub>4</sub> solution in the same potential window and at the same scan rate. Before the electrochemical measurements, the cell was bubbled with N<sub>2</sub> gas for at least 20 min and the N<sub>2</sub> gas flow was maintained over the solution surface during the measurements. All chemicals during this

work were an analytical reagent grade and the solutions were prepared from distilled water. The measurements were carried out at room temperature.

### 3. RESULTS AND DISCUSSION

#### 3.1. Physical and chemical characterization

##### 3.1.1. Chemical composition analysis

Metal atomic composition (Pt:Ru, atomic ratio) and weight percent determined by EDAX and the ICP are shown in Table (1). Pt:Ru is very closed to 1:1 atomic ratio which agrees with the nominal concentration of Pt and Ru in the starting precursor. During the EDAX analysis, no peaks for Cl or Na were observed, which insure that these undesirable elements were removed during the washing process. On the other hand, ICP analyses showed that the PtRu loading was 18 wt% for all catalysts which is near to the starting loading percentage of 20 % and confirms that almost all the Pt and Ru ions are reduced to their corresponding metallic state.

**Table 1.** Chemical composition of PtRu/C catalysts from EDAX and ICP-ASS Analyses

Catalysts Type	Reaction time hr	At % (from EDAX)		Wt % (From ICP-Ass)	
		Pt	Ru	Pt	Ru
PtRu/C1	1	47.59	52.41	11	7
PtRu/C2	2	48.05	51.95	11	7
PtRu/C4	4	45.11	54.89	11	7

##### 3.1.2. X-ray diffraction

Fig.(1) shows the X-ray diffraction patterns for the prepared catalysts, e.g. PtRu/C1, PtRu/C2 and PtRu/C3 respectively. X-ray diffraction analyses show that all catalysts exhibit the diffraction peaks of (111), (200), (220) and (311), respectively.

**Table (2):** Diffraction peaks for PtRu/C catalysts and pure Pt with their corresponding  $2\theta$  value

Catalysts Type	(111)	(200)	(220)	(311)
Pure Pt	39.7°	46.2°	67.4°	81.2°
PtRu/C1	39.8°	46.2°	67.8°	81.6°
PtRu/C2	39.8°	46.2°	67.7°	81.6°
PtRu/C4	39.9°	46.1°	67.8°	81.6°

These peaks are the characteristic for Pt face-centered cubic structure (f.c.c) (JCPDS Card No. 04-802). The wide peak near  $2\theta = 25^\circ$  corresponds to the diffraction of the carbon support (Vulcan

XC-72R). The diffraction peaks are located approximately at nearly  $2\theta$  values as that of pure metallic Pt as shown in Table 2. Since there is no shift of the diffraction peaks for higher  $2\theta$  value than that of pure Pt, no alloys formation or solid solution between Pt and Ru in the prepared PtRu/C can be detected which is in agree with the results of lattice constant calculated for all the prepared catalysts (Table. 3) [41].

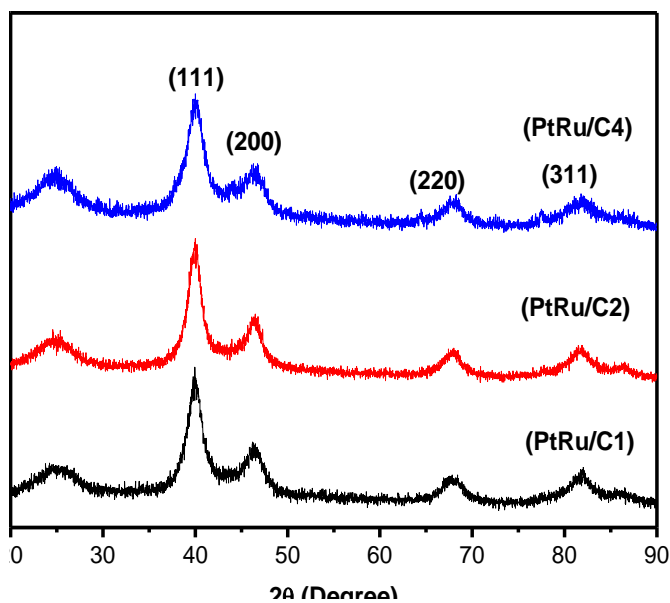


**Figure 1.** XRD patterns for PtRu/C catalysts prepared at different reaction time.

For the catalysts PtRu/C1 and PtRu/C2, there are no diffraction peaks characteristic for Ru or its oxide, even with the smooth profile obtained after elimination of the back ground and high frequency noise by the instrumental software. The same results are reported by many groups for PtRu/C catalysts [41-43] and this may be attributed to Pt that is decorated by Ru particles or may be Ru is present in amorphous phase or in form of hydrous Ru-oxide [43-46]. For PtRu/C4 catalyst, there is a new low intensity diffraction peak at about  $2\theta = 44^\circ$  between those of Pt (111) and (200). The peak was detected from the smooth profile of XRD pattern for PtRu/C4. This peak is the characteristic for (101) diffraction plane of Ru, most intense reflection plane for h.c.p Ru [46]. This suggests that in PtRu/C4, Ru is presence as a separate phase.

The particle size for all the prepared catalysts is calculated from the width of (220) diffraction peak using Gaussian fitting using Scherrer equation [42,43,47]:

$$D = \frac{0.95 \times \lambda}{\beta_{2\theta} \cos \theta_{\max}}$$

Where  $D$  is the particle size in (nm),  $\lambda$  is the wave length (0.15406 nm),  $\beta_{2\theta}$  is the fullwidth at half maxima in radius and  $\theta_{\max}$  is the angle at high maxima.

The lattice constant for the prepared catalysts was calculated from (220) diffraction peak by using Bragg law according to the following equation [42, 43]:

$$a_{fcc} = \frac{\sqrt{2}\lambda}{\sin \theta}$$

The particle size and the lattice constant for all prepared catalysts are given in Table (3). For all the prepared catalysts, the calculated particle size is nearly equal to about 3.7 and 3.8 nm which indicates that the particle size is slightly influenced by the reaction time.

Also, the lattice constants for all the catalysts are much closed to that of pure Pt which confirms that PtRu catalysts are present in unalloyed form.

The relative crystallinity of the prepared catalysts can be calculated from the ratio between the height peak of Pt (111) and peak reflection of the carbon. These values of relative crystallinity are given in Table (3). From Table (3), catalysts PtRu/C2 has a higher crystallinity than that of PtRu/C1 and PtRu/C4.

**Table 3.** The structural parameters for PtRu/C catalysts from XRD analysis and average particle size from TEM calculations.

Catalysts type	Particle size	Lattice constant	Relative crystallinity	Average
	XRD (nm)	(nm)		particle size
				TEM (nm)
PtRu/C1	4.9	0.3906	4.85	3.7
PtRu/C2	4.9	0.3908	5	3.7
PtRu/C4	4.7	0.3906	3	3.8
PtRu/C [38].	-	-	-	6.96

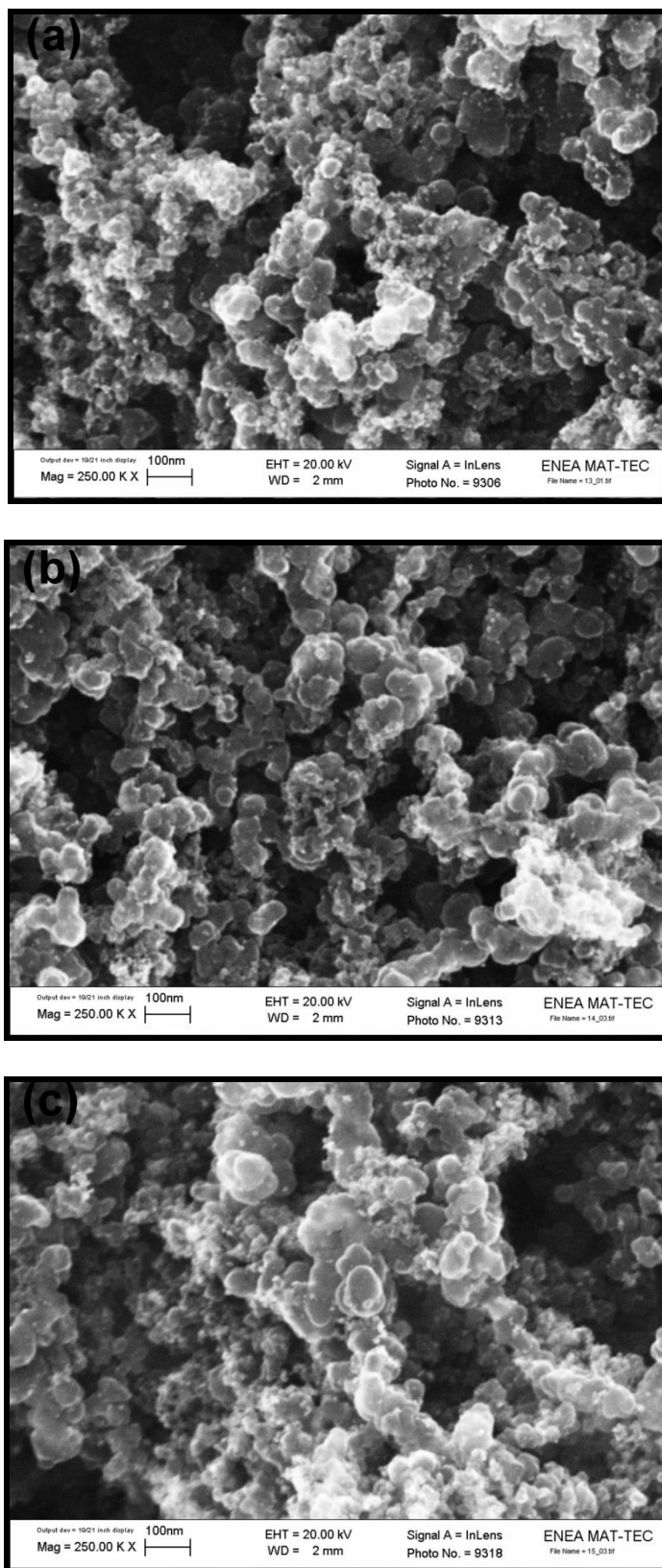
### 3.1.3. FESEM and TEM analysis

Fig (2) and Fig (3) show the FESEM and TEM images of the synthesized PtRu/C catalysts. From both FESEM and TEM images we observe the deposits of PtRu nanoparticles on the carbon support. The nanoparticles are in good dispersion on the support.

For PtRu/C4, the presence of large amount of agglomeration is observed and some of the carbon particles were not covered by PtRu nanoparticles.

The histograms for particle size distribution are shown in Fig (3). The average particle sizes were 3.7, 3.7, 3.8 for PtRu/C1, PtRu/C2, PtRu/C4; respectively.

The average particle for PtRu/C catalysts reported in this work is smaller than that reported by Lee et al using the same preparation method, which was 6.96 nm and 10.2 nm upon addition of 1M NaOH. [38]



**Figure 2.** FESEM photographs for PtRu/C catalysts (PtRu/C1;(a), PtRu/C2; (b), PtRu/C4; (c).

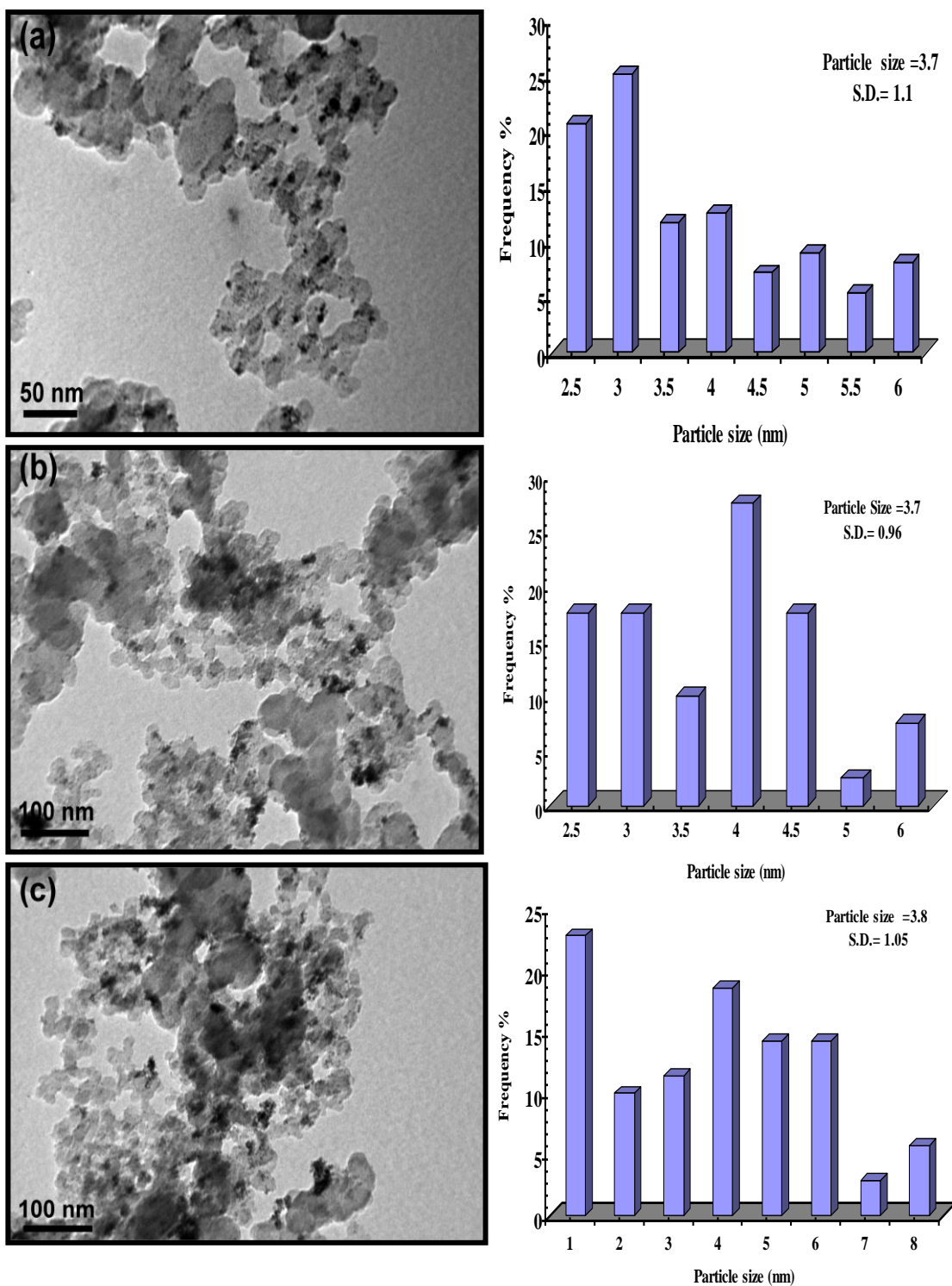


**Figure 3.** TEM photographs for PtRu/C catalysts (PtRu/C1;(a), PtRu/C2; (b), PtRu/C4; (c)) and the corresponding histograms.

### 3.2. Electrochemical measurements

The cyclic voltammograms for PtRu/C catalysts in H<sub>2</sub>SO<sub>4</sub> are shown in Fig (4, column A). The PtRu/C1 and PtRu/C4 showed the typical behavior of Pt electrode in H<sub>2</sub>SO<sub>4</sub> with peaks in hydrogen

adsorption-desorption region (-0.2– 0.15 V vs. SCE) and a peak for PtO<sub>x</sub> reduction in the reverse scan. The characteristic peaks were well defined in case of PtRu/C1 than that on PtRu/C4. It appears from these characteristics that the two catalysts have Pt-rich surface. On the other hand, for PtRu/C2, the H-desorption peaks are very low and the peak for PtO<sub>x</sub> is suppressed completely. It is reported that the behavior of Pt catalyst electrode in H<sub>2</sub>SO<sub>4</sub> is affected by the incorporation of Ru and its percent on the surface and PtRu catalysts with 50 At. % doesn't show the same behavior of Pt catalysts. The suppressed of hydrogen desorption process in PtRu/C2 may be attributed to the formation RuO<sub>x</sub> at lower potential and it could be due to the presence of hydrous Ru-oxide [45].

The CV's for methanol oxidation on all prepared catalysts electrodes are shown in Fig (4, column B). All cyclic voltammograms are similar to methanol oxidation voltammograms reported in the literature [32, 46], with the peak for oxidation of methanol in the forward scan and another peak in backward scan characteristic for oxidation of intermediate adsorbed on the electrode surface in the forward scan. For the PtRu/C4, the peak potential for methanol oxidation is shifted for higher potential than that of other catalysts. This may be attributed to the agglomeration of nanoparticles catalysts as it detected by FESEM and TEM. The high dispersion and uniform distribution of nanoparticles catalysts in the carbon supports could enhance the electrocatalytic activity of the nanocatalysts. The electrocatalytic activities for all the catalysts are evaluated using mass specific activity (MSA) and peak potential for methanol electrooxidation. The MSA was calculated by integration of the charge density corresponding for methanol oxidation divided by metal loading according to the following equation [48-50]:

$$MSA = \frac{Q_{MOR}}{L_{PtRu}}$$

Where the MSA is the mass specific activity for MOR (mCmg<sup>-1</sup>),  $Q_{MOR}$  is the charge density for methanol oxidation peak (mC/cm<sup>2</sup>) and  $L_{PtRu}$  is the loading of PtRu in the electrode (mg/cm<sup>2</sup>)

The values for mass specific activities for all catalysts electrodes at steady state (after 50 cycles) and the peak potential for methanol electrooxidation are shown in Table (4).

**Table 4.** Mass specific activities for PtRu/C catalysts

Catalysts type	MSA (mCmg <sup>-1</sup> )	CH <sub>3</sub> OH oxidation peak potential (V)
PtRu/C1	175	0.69
PtRu/C2	196	0.68
PtRu/C4	165	0.75

PtRu/C2 showed higher MSA which indicates that the electrode fabricated from this catalyst has higher electrocatalytic activity towards methanol electro-oxidation reaction. This higher electrocatalytic activity of PtRu/C2 could be attributed to high dispersion or more homogenous of nanoparticles catalysts on the support and the formation of hydrous ruthenium oxide. It is reported that the hydrous ruthenium oxide has promoter effect in PtRu catalysts more than that the Ru alloyed in PtRu [51]

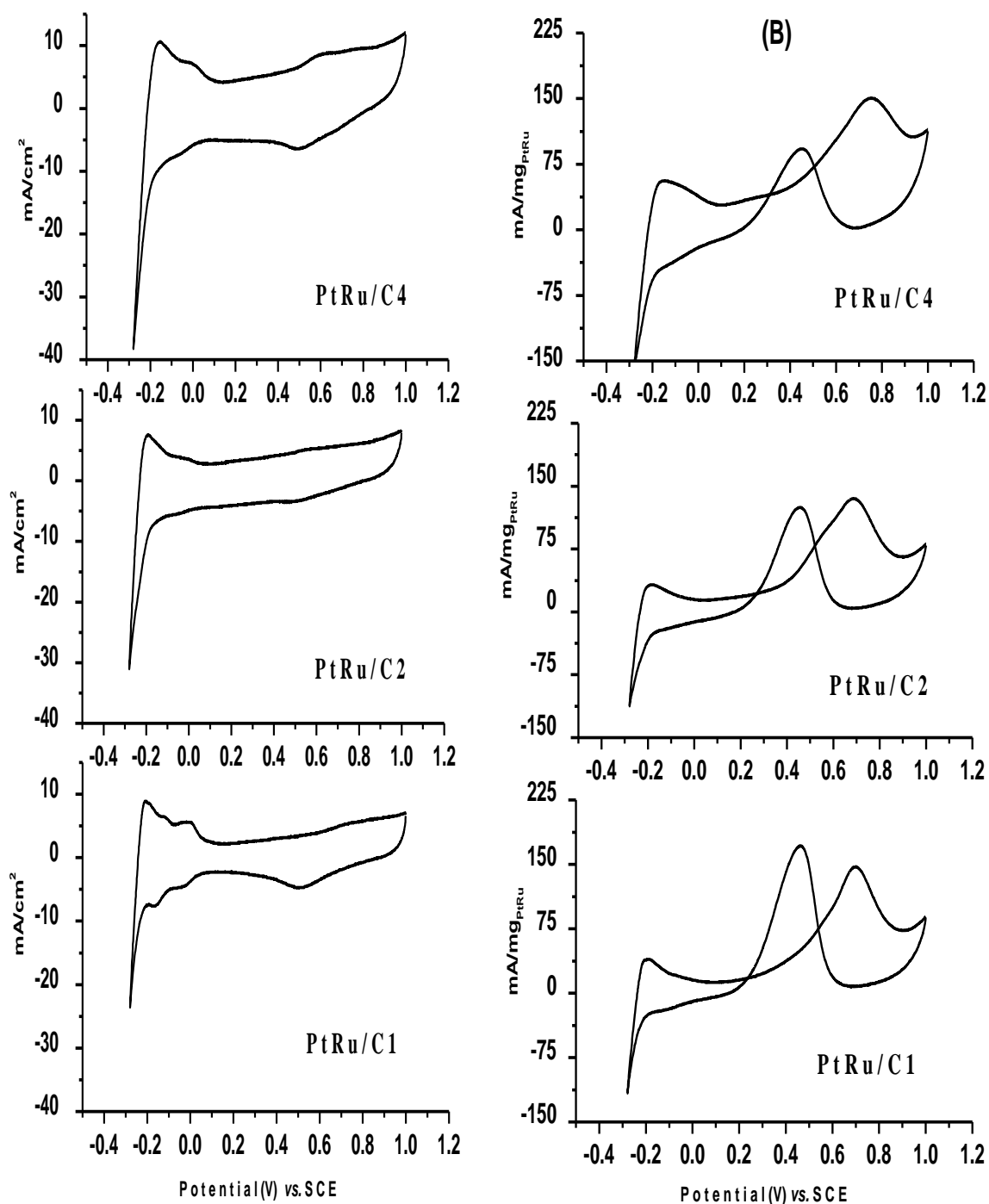


**Figure 4.** Cyclic voltammograms for PtRu/C electrocatalysts in 1M H<sub>2</sub>SO<sub>4</sub> (column, A) and 0.5M CH<sub>3</sub>OH/1M H<sub>2</sub>SO<sub>4</sub> (column, B) (scan rate 100 mV/sec).

For methanol electro-oxidation potential peaks, PtRu/C2 showed lower peak potential among all catalysts which indicate that this catalyst has good electrocatalytic activity for methanol electrooxidation. On the other side, PtRu/C4 showed higher peak potential which could be attributed to the presence of large agglomeration in this catalyst that could retard the oxidation of methanol at lower potential. The peak potentials for methanol oxidation on the catalysts prepared in this work are very

closed to the peak potential for methanol oxidation on PtRu supported on acid functionalized carbon nanotubes (PtRu/CNTs) reported by Chetty *et.al.* and prepared by impregnation in ethanol followed by reduction at high temperature with flow of hydrogen and helium[46].

To test the durability and stability of electrode catalysts to be applicable in DMFCs, all electrodes were cycled in methanol for 100 cycles of potential sweep. The MAS activities for all electrodes against cycle number of potential sweep are plotted in Fig (5). PtRu/C1 showed a decay for MSA and it decreases rapidly with increasing the cycle number. On the other hand for other electrodes, the MSA activities start low but increases with cycling, which is an indication that the cycling process activates the electrode for methanol oxidation by adsorption of more methanol molecules and then the MSA is extremely stabilized. From Fig (5) we can detect that PtRu/C2 has higher MSA and good stability, which futures this catalyst to be a promising catalyst electrode for methanol electro-oxidation in DMFCs.

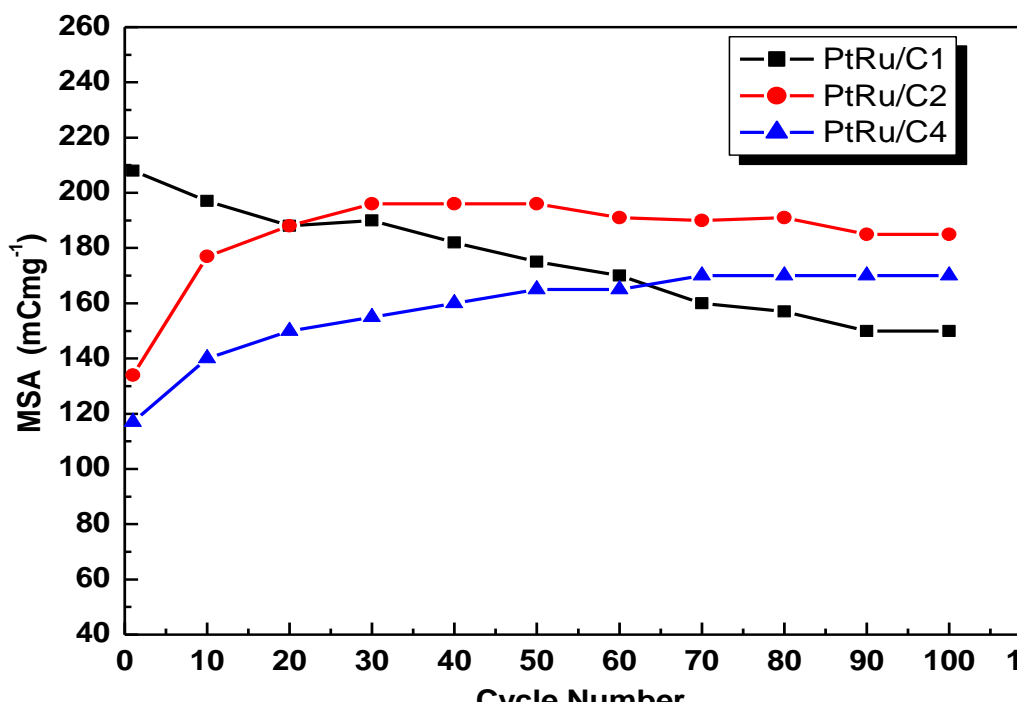


**Figure 5.** The MSA activities for PtRu/C catalysts electrodes as function of cycle number of potential sweep in 0.5M CH<sub>3</sub>OH/1M H<sub>2</sub>SO<sub>4</sub>.

#### 4. CONCLUSIONS

The carbon supported PtRu nanocatalysts have been synthesized using a simple impregnation reduction method in ethanol as solvent and reducing agent at the same time. The XRD characterization showed that all catalysts exhibit f.c.c structure phase and only Ru h.c.p structure phase can be detected at higher reaction time. From lattice constant calculations, the prepared catalysts are present in unalloyed form.

The PtRu nanoparticles showed a good dispersion on the support and the average particle size was in range of 3.7 nm with narrow particles distribution for PtRu/C prepared at 2h (PtRu/C2). The electrocatalytic activities of nanocatalysts evaluated in terms of mass specific activity. Among all catalysts, PtRu/C2 showed higher electrocatalytic activity for methanol electro-oxidation. This work indicate how the reaction time and therefore the morphological feature influence the electrocatalytic activity despite that all catalysts almost have the same crystal structure and the particle size. An optimum reaction time of 2h was able to produce nanoparticles with good dispersion and narrow particle size distribution which enhance the catalytic activity. The work demonstrates that ethanol impregnation reduction method is simple and low cost method for preparation of nanocatalysts as promising materials for application in direct methanol fuel cells.

#### ACKNOWLEDGMENTS

The authors are provided thanks for Emanuele Serra and Elena Salernitano, ENEA, Casaccia Research Centre, for the FESEM analyses and for help during the work. One of the authors, Abu Bakr A.A. Nassr is grateful thanks for Abdus Salam International Centre for Theoretical Physics (ICTP) and International Italian Agency for New Technologies; Energy and Environment (ENEA) for (ICTP-ENEA) fellowship on Training and Research in Italian Laboratories programme (TRIL- programme).

#### References

1. E. L. Gyenge, Chapter 4: 'Electrocatalytic oxidation of methanol, ethanol and formic acid', in PEM Fuel Cell Electrocatalysts and Catalyst Layers, editor; JiuJun Zhang, Springer, New York, p. 165-270 (2008).
2. A. O. Neto, R. W. R. Verjullo-Silva, M. Linardi and E.V. Spinacé, *Int. J. Electrochem. Sci.*, 4 (2009) 954.
3. A. B. Kashyout, A. A. A. Nasr, M. S. Mohy Eldin, *Alexandria Engineering Journal*, 48 (2009) 491.
4. G.T. Burstein, C.J. Barnett, A.R. Kucernak, K.R. Williams; *Catal. Today* 38 (1997) 425.
5. T. Iwasita, *Electrochim. Acta* 47 (2002) 3663.
6. M. Brandalise, M. M. Tusi, R. M. Piasentin, M. Linardi, E.V. Spinacé, A. O. Neto, *Int. J. Electrochem. Sci.*, 5 (2010) 39.
7. H. Liu, C. Song, L. Zhang, J. Zhang, H. Wang, D.P. Wilkinson; *J. Power Sources* 155 (2006) 95.
8. W. M. Martínez, T. T. Thompson, M. A. Smit, *Int. J. Electrochem. Sci.*, 5 (2010) 931.
9. A. Hamnett; *Catal. Today* 38 (1997) 445.
10. J.L. Gómez de la Fuente, M.V. Martínez-Huerta, S. Rojas, P. Terreros, J.L.G. Fierro, M.A. Pena; *Catal. Today* 116 (2006) 442.
11. E.A. Bagotski, Y.B. Vassiliev, O.A. Khazova, *J. Electroanal. Chem.* 81 (1977) 229.
12. G. Stalnionis, L. Tamasauskaite-Tamasiunaite, V. Pautieniene, A. Sudavicius, Z. Jusys, *J. Solid State Electrochem.* 8 (2004) 892.
13. B. Gurau, R. Viswanathan, R. Liu, T.J. Lafrenz, K.L. Ley, and E. S. Smotkin, E. Reddington, A. Sapienza, B.C. Chan, T.E. Mallouk, S. Sarangapani, *J. Phys. Chem. B* 102(1998) 9997.
14. Z. Liu, J.Y. Lee, W. Chen, M. Han, L.M. Gan, *Langmuir* 20(2004) 181.
15. T. Maiyalagan *Int. J. Hyd. Energy.* 34 (2009) 2874.
16. T. Maiyalagan, *J Solid State Electrochem* 13 (2009) 1561.
17. S. Jingyu, H. Tianshu, C. Yanxia, Z. Xiaogang, *Int. J. Electrochem. Sci.* 2 (2007) 64.
18. A.O. Neto, R.R. Dias, M.M. Tusi, M. Linardi, E.V. Spinacé, *J. Power Sources* 166(2007) 87.

19. H.B. Hassan *J. Fuel Chem. Tech.* 37 (2009) 346.
20. T. C. Deivaraj, W. Chen and J.Y. Lee. *J. Mater. Chem.*, 13 (2003) 2555.
21. Z. C.Wang, Z.M.Ma, H.L. Li, *Appl. Surf. Sci.*, 254 (2008) 6521.
22. S. A. Lee, K.W.Park, J.H. Choi, B.K. Kwon, Y. E.Sung, *J. Electrochem. Soc.*, 149 (2002) A1299.
23. T. Y. Morante-Catacora, Y. Ishikawa, C. R. Cabrera, *J. Electroanal. Chem.* 621 (2008) 103.
24. M. V. Martínez-Huerta, S. Rojas, J.L. Gómez de la Fuente, P. Terreros, M.A. Peña, J.L.G. Fierro *Appl. Catal. B: Environ.*, 69 (2006) 75.
25. S. Pasupathi, V. Tricoli, *J. Solid State Electrochem.* 12 (2007)1093.
26. T. Huang, J. Liu, R. Li, W. Cai, A. Yu, *Electrochem. Commun.* 11(2009) 643.
27. A. Oliveira Neto, E.G. Franco, E. Aricó, M. Linardi, *Portug. Electrochim. Acta* (2004) 93.
28. Z. B.Wang<sup>1</sup>, P.J. Zuo, G.P. Yin *Fuel Cells* 9 (2009) 106.
29. T. Maiyalagan, B. Viswanathan, U.V. Varadaraju, *J. Nanosci. Nanotechnol.* 6 (2006) 2067.
30. T. Maiyalagan, B. Viswanathan *J. Power Sources* 175 (2008) 789.
31. T. Maiyalagan, F.N. Khan, *Catal. Commun.* 10 (2009) 433.
32. C. Zhou, H. Wang, F. Peng, J. Liang, H. Yu, J. Yang, *Langmuir*, 25(2009) 7711.
33. T. Frelink, W. Visscher, J.A.R. van Veen *Surface Science* 335 (1995) 353-360.
34. K. Y.Chan, J. Ding, J. Ren, S.Cheng, K.Y.Tsang, *J. Mater. Chem.*, 14 (2004) 505.
35. T. K. Sau, M. Lopez, D.V. Goia, *Chem. Mater.* 21 (2009) 3649.
36. R. Richard, H. Bonnemann, Chapter 10: Nanomaterials as Precursors for Electrocatalysts in Catalysis and electrocatalysis at nanoparticles Surfaces, Edited by A.Wieckowski, E.R. Savinova, C.G. Vayenas, Marcel Dekker, New York, 2003, pp343.
37. J. Prabhuram, X. Wang, C. L. Hui, and I.M. Hsing, *J. Phys. Chem. B*, 107 (2003) 11057.
38. T. C. Deivaraj, J. Y. Lee, *J. Power Sources* 142 (2005) 43.
39. B. R. Camacho<sup>1</sup>, M. T. Rodríguez<sup>1</sup> and O.S.Feria, *J. New Mat. Electrochem. Systems.* 12 (2009) 43.
40. M. J. Swain and D. H. Ballard, "Color Indexing", *Intl. J. of Computer Vision*, 7 (1991) 11.
41. W. H. Lizcano-Valbuena, V.A. Paganin, E.R. Gonzalez, *Electrochim. Acta*, 47 (2002) 3715.
42. J. W. Guo, T.S. Zhao, J. Prabhuram, R. Chen, C.W. Wong, *Electrochim. Acta*, 51 (2005) 754.
43. T. Vidakovic, M. Christov, K. Sundmacher, K.S. Nagabhushana, W. Fei, S. Kinge, H. Bonnemann, *Electrochim. Acta*, 52 (2007) 2277.
44. E. Antolini, F. Cardellini, L. Giorgi, *J. Mater. Sci. Lett.* 19 (2000) 2099.
45. E.G. Franco, A.O. Neto, M. Linardi, E. Aricó, *J. Braz. Chem. Soc.*, 13 (2002) 516.
46. R.Chetty, W. Xia, S. Kundu, M. Bron, T. Reinecke, W. Schuhmann, M. Muhler, *Langmuir* 25 (2009) 3853.
47. L. Giorgi, A. Pozio, C. Bracchini, R. Giorgi, S. Turtu, *J. Appl. Electrochem.*, 31 (2001) 325.
48. L. Giorgi, T.D. Markis, R. Giorgi, N. Lisi, E. Salernitano, *Sens. Actuat. B*, 126(2007)144.
49. C. Paoletti, A. Cemmi, L. Giorgi, R. Giorgi, L. Pilloni, E. Serra, M. Pasquali, *J. Power Sources*, 183(2008) 84.
50. D. M. Gattia, M. V. Antisari, L. Giorgi, R. Marazzi, E. Piscopiello, A. Montone, S. Bellitto, S. Licoccia, E. Traversa, *J. Power Sources* 194 (2009) 243.
51. J. W. Long, R.M. Stroud, K.E.S. Lyons, D.R. Rolison, *J. Phys. Chem. B* 104 (2000) 9772.